Hindawi Publishing Corporation
International Journal of Antennas and Propagation
Volume 2014, Article ID 847475, 8 pages
http://dx.doi.org/10.1155/2014/847475

Research Article

Two-Element Tapered Slot Antenna Array for Terahertz Resonant Tunneling Diode Oscillators

Jianxiong Li,[1] Yunxiang Li,[1] Weiguang Shi,[1] Haolin Jiang,[1] and Luhong Mao[2]

[1] *School of Electronics and Information Engineering, Tianjin Polytechnic University, Tianjin 300387, China*
[2] *School of Electronic Information Engineering, Tianjin University, Tianjin 300072, China*

Correspondence should be addressed to Jianxiong Li; lijianxiong@tjpu.edu.cn

Received 23 June 2014; Revised 29 August 2014; Accepted 3 September 2014; Published 14 October 2014

Academic Editor: Jaume Anguera

Two-element tapered slot antenna (TSA) array for terahertz (THz) resonant tunneling diode (RTD) oscillators is proposed in this paper. The proposed TSA array has the advantages of both the high directivity and high gain at the horizontal direction and hence can facilitate the horizontal communication between the RTD oscillators and other integrated circuit chips. A MIM (metal-insulator-metal) stub with a T-shaped slot is used to reduce the mutual coupling between the TSA elements. The validity and feasibility of the proposed TSA array have been simulated and analyzed by the ANSYS/ANSOFT's High Frequency Structure Simulator (HFSS). Detailed modeling approaches and theoretical analysis of the proposed TSA array have been fully addressed. The simulation results show that the mutual coupling between the TSA elements is reduced below −40 dB. Furthermore, at 500 GHz, the directivity, the gain, and the half power beam width (HPBW) at the *E*-plane of the proposed TSA array are 12.18 dB, 13.09 dB, and 61°, respectively. The proposed analytical method and achieved performance are very promising for the antenna array integrated with the RTD oscillators at the THz frequency and could pave the way to the design of the THz antenna array for the RTD oscillators.

1. Introduction

The terahertz (THz) frequency, ranging from 100 GHz to 10 THz, has recently attracted a large number of interests in lots of applications, such as radio astronomy, biological monitoring, nondestructive evaluation, and information and communications technology (ICT) [1–4]. To realize the applications above, the resonant tunneling diodes (RTDs) have been seen as good candidates for the THz oscillators working at room temperature [5–7]. In addition, the good antenna is also considered as the key component for THz oscillators, which can improve the sensitivity of the oscillators to one to two orders of magnitude.

Among the various implementations of antennas integrated with the RTD oscillators, the patch antennas including the rectangular patch antenna [8] and the circular patch antenna [9] have the advantage of achieving the oscillation frequency at the THz band without using the Si lens. Besides, the offset-fed slot antenna, introduced by Hinata et al. [10] and implemented by having the feeding point deviated from the center of the slot antenna, has drawn considerable attention due to the fact that the oscillator has a high output power of 200 uW with the potential of oscillating up to 2 THz. The antennas above designed in planar structure have the vertical radiation pattern. However, in some special applications, such as the wireless data transmissions, an antenna with the horizontal radiation pattern applicable to the horizontal communication is preferable. Thus, the tapered slot antennas (TSAs) are ideal options since they can maintain the directivity approximate to horn antennas. At present, most researches on TSAs are concentrated on the millimeter wave band [11–14]. Very recently, the TSA working at 405 GHz was reported in [15], whose directivity is 8.9 dB. However, the main content of [15] is centered on the RTD, and there is little information and theoretical analysis about how the TSA is designed and matched with the RTD.

The output power of the RTD oscillators integrated with the antenna is usually low (~uW level) [8–10, 16–19]. To improve the output power, designing antennas with high directivity and high radiation efficiency is one effective way. Furthermore, the design of the antenna array which can achieve the output power combination of the RTD oscillators

is another effective method. Recently, the offset-fed slot antenna array for the RTD oscillators is reported in [20], which achieves the individual output powers of 1.9 uW at 329 GHz and 2.6 uW at 332 GHz, respectively. When the two oscillators are driven simultaneously, a single peak output power of 5.1 uW is obtained at 321 GHz, which is little larger than the summation of the individual output power. This outcome is rather significant in obtaining the high output power of the RTD oscillators, which illustrates the feasibility of the design of the oscillators array. However, there is little information about the modeling approaches and simulation results of the antenna array.

In this paper, the detailed modeling approaches and theoretical analysis of a high directivity and high gain TSA array for THz RTD oscillators are proposed. To our knowledge, this is the first time to apply the TSA array integrated with the RTD oscillators. The matching conditions between the RTD and the TSA element have been fully considered and addressed. The MIM (metal-insulator-metal) stub with a T-shaped slot is used to reduce the mutual coupling between the TSA elements. The validity and feasibility of the proposed TSA array have been simulated and analyzed by ANSYS/ANSOFT's High Frequency Structure Simulator (HFSS). The simulation results show that the directivity and the gain of the TSA array have been greatly improved compared with the TSA element. Furthermore, the mutual coupling between the TSA elements has been greatly reduced, and the side lobes of the proposed TSA array have been greatly supressed. The proposed analytical method and achieved performance are very promising for the antenna array integrated with the RTD oscillators at the THz frequency and could pave the way to the design of the THz antenna array for the RTD oscillators.

2. Theoretical Analysis of the TSA Element

The TSAs belong to the class of directional antennas known as surface-wave antennas, which utilize a traveling wave propagating along the antenna structure with a phase velocity $v_{\text{ph}} < c$. The TSAs maintain the advantage of producing symmetric radiation patterns in the planes which are parallel to the substrate (E-plane) and perpendicular to the substrate (H-plane), though their geometries are completely planar. To work as a surface-wave antenna, the effective substrate thickness (t_{eff}) of the TSA has to obey the following requirement [21]:

$$0.005 < \frac{t_{\text{eff}}}{\lambda_0} = \left(\sqrt{\varepsilon_r} - 1\right)\frac{t}{\lambda_0} < 0.03, \tag{1}$$

where λ_0 is the free-space wavelength, ε_r is the relative dielectric constant of the substrate, t is the substrate thickness. The beam width will get wider by using a thinner substrate. Thus, it is vital to know the upper limit of the substrate thickness.

A standard TSA consists of a tapered radiating slot used as a transformer to the free space. Among the various types of the TSAs, the most common are the linearly tapered slot antenna (LTSA), the exponential tapered slot antenna (ETSA), and the constant-width tapered slot antenna (CWSA) [22]. Usually, the beam width of the CWSA is the narrowest, followed by LTSA and ETSA on the condition of the same substrate with the same length and aperture size. However, the situation described above is opposite for the side lobe level. Thus, the LTSA is an ideal compromise due to considering the beam width and the side lobe level.

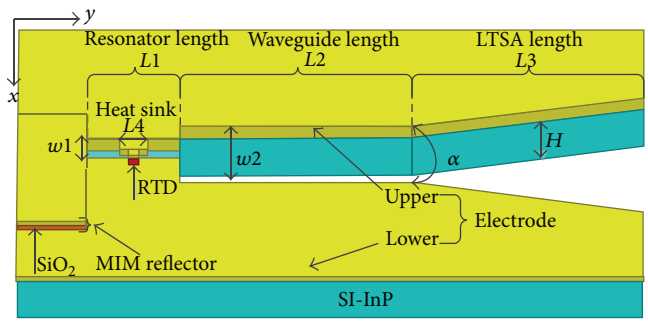

Figure 1: Schematic structure of the proposed TSA element.

The radiation of the LTSA is restricted into the slot by the metal surface; thus, the propagation is end-fire. The bandwidth of the LTSA is decided by the maximal and minimal distance of the slot. The directivity can be estimated as

$$D = \frac{4}{\int_0^{\pi}\left(\left|F_E(\theta)\right|^2 + \left|F_H(\theta)\right|^2\right)\sin\theta\, d\theta}, \tag{2}$$

where $F_E(\theta)$ and $F_H(\theta)$ are, respectively, the directivity function of the E-plane and the H-plane.

The schematic structure of the proposed RTD-integrated TSA element is demonstrated in Figure 1, which is not the same proportion as the real size. The whole device is composed of a resonator, a waveguide, and an LTSA. A double-barrier RTD is located in the resonator. The upper and lower electrodes of the TSA element are connected to the correspondent sides of the RTD. For heat sink, the bridge connects the upper edge of the RTD and the upper electrode is designed much larger than the RTD. At one end of the resonator, a 100-nm-thick SiO_2 is inserted between the upper and lower electrodes to prevent short. The waveguide with a slightly larger width is linked to the other end of the resonator; thus, the standing wave is formed since the high frequency electromagnetic waves are reflected at the both edges of the resonator. Finally, the THz wave is radiated horizontally through the waveguide and the LTSA.

The resonator can be equivalent to an offset-fed slot antenna integrated with RTD. For the antenna without offset, the resonant point should satisfy the following conditions [23]:

$$\frac{\lambda_0}{2n_e} \times n = l,$$
$$n_e = \left(\frac{\varepsilon_r + 1}{2}\right)^{-1/2}, \tag{3}$$

where l is the length of the offset-fed slot antenna, n_e is the equivalent refractive index, and n is a positive integer.

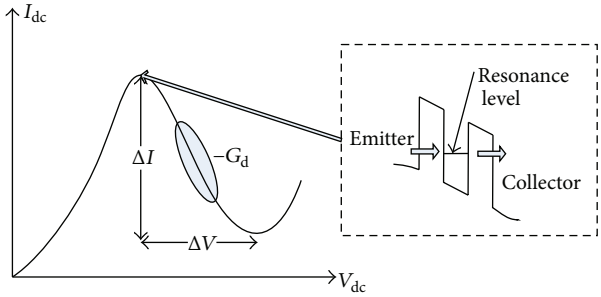

Figure 2: Potential profile and characteristics of RTD.

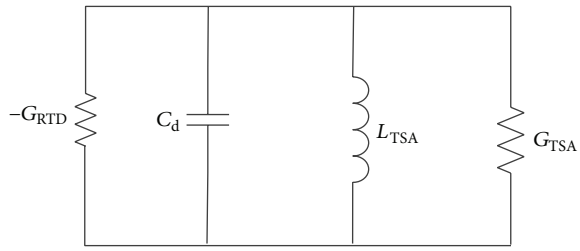

Figure 3: Equivalent circuit of TSA element integrated with RTD without parasitic elements.

The impedance of the TSA element increases with the increasing of the resonator width, and the resonant frequency decreases with the increasing of the resonator length.

The potential profile and characteristics of the RTD are shown in Figure 2; we can observe that the RTD is composed of two heterobarriers and a quantum well. In the current-voltage (I-V) characteristics, the resonance level in the quantum well is close to the conduction band edge of the emitter at the peak current. With the increasing of the voltage above the peak current, a negative differential conductance (NDC) region exists, which corresponds to the negative differential resistance (NDR) region. The oscillation of the RTD integrated with the antenna is obtained in this region [24]. Therefore, because of the NDR of the RTD and the positive resistance of the antenna, the conjugate impedance matching condition between the RTD and the antenna is rather difficult. Generally, the matching conditions are analyzed through the equivalent circuit mode.

The oscillation of the RTD oscillators integrated with the antenna can be achieved if the following two conditions are met simultaneously [25]:

$$\begin{aligned} \mathrm{Re}\,(Y) &\le 0, \\ \mathrm{Im}\,(Y) &= 0, \end{aligned} \tag{4}$$

where Y is the total admittance of the antenna and the RTD.

The equivalent circuit of the proposed TSA element integrated with RTD without parasitic elements is expressed as shown in Figure 3. The parasitic elements such as the resistance and capacitance of the upper contact of the RTD, the inductance of the RTD mesa, the mesa resistance, and the spreading resistance from the RTD mesa to the lower electrode can be neglected here, which does not affect the conclusions of the analysis. C_d is the inherent capacitance of the RTD, L_{TSA} is mainly determined by the TSA element. $-G_{RTD}$ is the negative differential conductance (NDC) of the RTD, G_{TSA} is the conductance of the TSA which represents the radiation loss of the TSA element. Oscillation occurs if $G_{RTD} > G_{TSA}$; that is, the absolute value of the NDC exceeds the radiation loss of the TSA element.

Usually, the output power of the RTD oscillators integrated with the antenna is low (~uW level). By an approximate analysis, the output power is given as [26]

$$P = \frac{G_{ANT} \times (G_{RTD} - G_{ANT})\,\Delta V^2}{2G_{RTD}}, \tag{5}$$

where P can be maximized at the condition $G_{ANT} = G_{RTD}/2$, where G_{ANT} is equal to the G_{TSA} in this paper. Furthermore, if the tunneling time and transit time are neglected, the maximum value of the output power will be obtained as [27]

$$P_{max} = \frac{3}{16}\Delta I \Delta V, \tag{6}$$

where ΔI and ΔV are the current and voltage of the NDR region.

Table 1: Specifications of the proposed TSA element.

Parameters	Value
Design frequency	500 GHz
10 dB bandwidth	>200 GHz
Peak directivity	>9.0 dB
Radiation efficiency	>80%
HPBW	>50°
Front back to ratio	>10 dB

3. Design of the TSA Element

So far, there is no unified standard about the design of the THz antenna for RTD oscillators. Several factors which are rather important for the antenna should be fully considered. First, the antenna should have high directivity and high radiation efficiency for improving the output power of the RTD oscillators, as mentioned above. Furthermore, antennas with broadband are also necessary which can broaden the range of the application for the RTD oscillators. Other factors such as the half power beam width (HPBW) and the front back to ratio are also crucial for designing the antennas for RTDs oscillators. The design specification of the proposed TSA element is shown in Table 1.

The proposed TSA is designed on the semi-insulting (SI) InP substrate. The equivalent refractive index of SI-InP and SiO_2 are 3.48 and 1.97, and their conductances are neglected. The substrate is thinned in order to reduce the radiation loss of the substrate. It is assumed that both electrodes are made of gold ($\sigma = 4.52 \times 10^7$ S/m), and the frequency dependence of the conductivity is neglected. The mesh area of the RTD is $4\,\mu m^2$, which is linked to the RTD and the heat sink. Considering the design specification, the parameters of the proposed TSA element are shown in Table 2.

Table 2: Parameters of the proposed TSA element.

Parameters	Value
$L1$	35 um
$L2$	890 um
$L3$	890 um
$L4$	6 um
$w1$	8 um
$w2$	36 um
H	20 um
α	15°

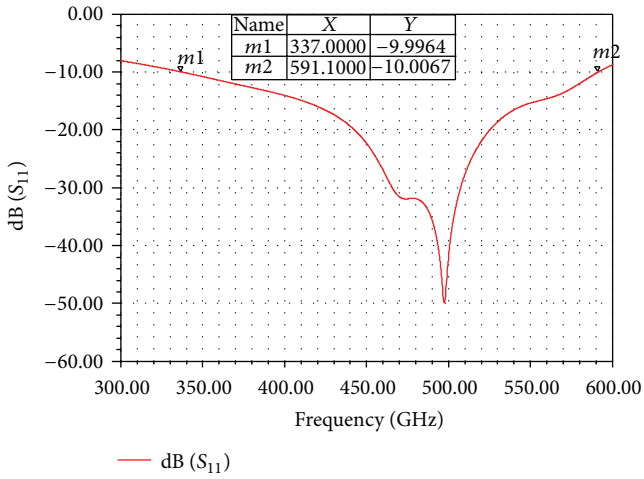

Figure 4: Return loss of the proposed TSA element.

By the circuit simulation, the NDC of the RTD is −6.52 mS at 500 GHz and the inherent capacitance C_d is 3.8 fF. Thus, theoretically, the admittance of the proposed TSA element is $(3.26 - j * 11.84)$ mS, and the corresponding impedance is $(21.6 + j * 78.5)$ ohm at 500 GHz.

The return loss and the impedance versus frequency of the proposed TSA element are shown in Figures 4 and 5, respectively. We can observe that the bandwidth of the proposed TSA is 254 GHz (from 337 GHz to 591 GHz, $S_{11} < -10$ dB), which yields a rather large relative bandwidth of 54.7%. Furthermore, the impedance of the proposed TSA element is $(22.0 + j * 79.8)$ ohm at 500 GHz, with the corresponding admittance of $(3.2 - j * 11.6)$ mS, both of which agree very well with the theoretical values.

The radiation pattern and the directivity at the E-plane of the proposed TSA element at 500 GHz are shown in Figures 6 and 7, respectively. We can observe that the gain, the directivity, and HPBW at the E-plane of the proposed TSA element are 9.58 dB, 10.38 dB, and 59°, respectively. Furthermore, the first side lobe's gain is −1.89 dB at $\theta = 39°$, the front back to ratio is 11.5 dB, and the radiation efficiency is 83.2%.

From the analysis of the proposed TSA element above, we can obtain that the proposed TSA element enjoys a broadband centered at 500 GHz, high directivity, and high gain at the horizontal direction, which satisfies the design

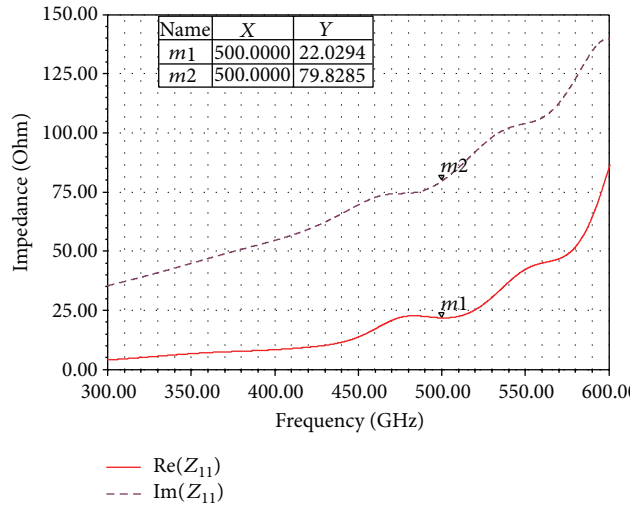

Figure 5: Impedance of the proposed TSA element.

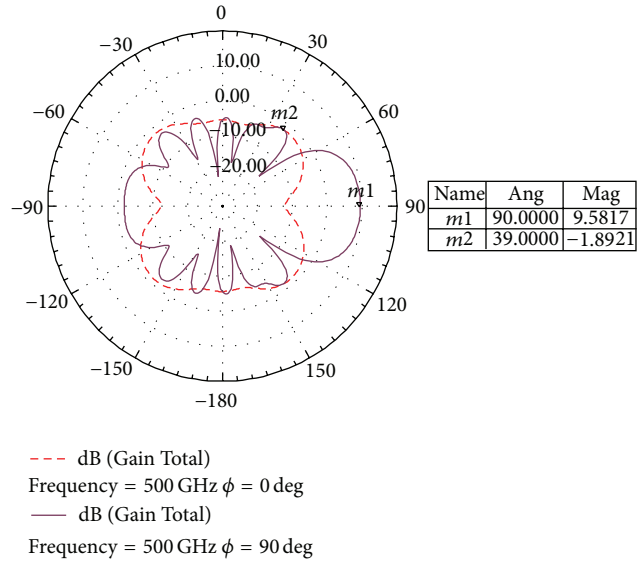

Figure 6: Radiation pattern of the proposed TSA element at 500 GHz.

specification of the TSA element and lays a good foundation for the design of the TSA array. The problems of the next stage work are to reduce the mutual coupling between the TSA elements and suppress the side lobes of the TSA array.

4. Design and Theoretical Analysis of the TSA Array

The schematic structure of the proposed TSA array integrated with the RTDs is demonstrated in Figure 8. Two TSA elements are designed linearly in a planar. The MIM stub with a T-shaped slot is used to reduce the mutual coupling between the TSA elements. The schematic structure of the coupling part is shown in Figure 9. The coupling part length $L5$ is 100 μm, which is less than a quarter of the wavelength.

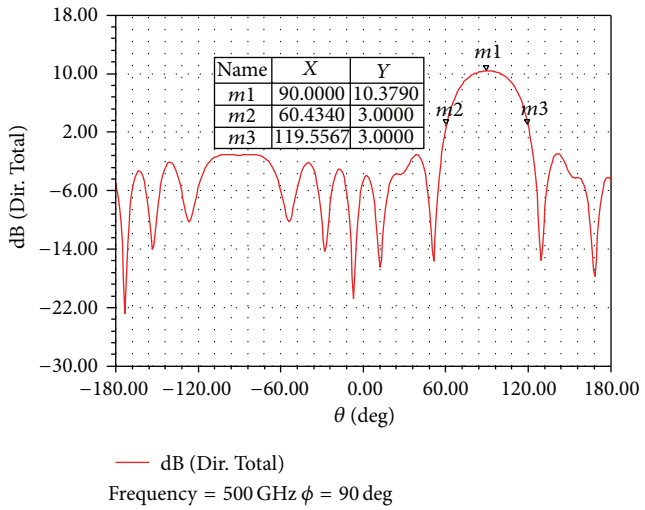

Figure 7: Directivity of the proposed TSA element at the E-plane at 500 GHz.

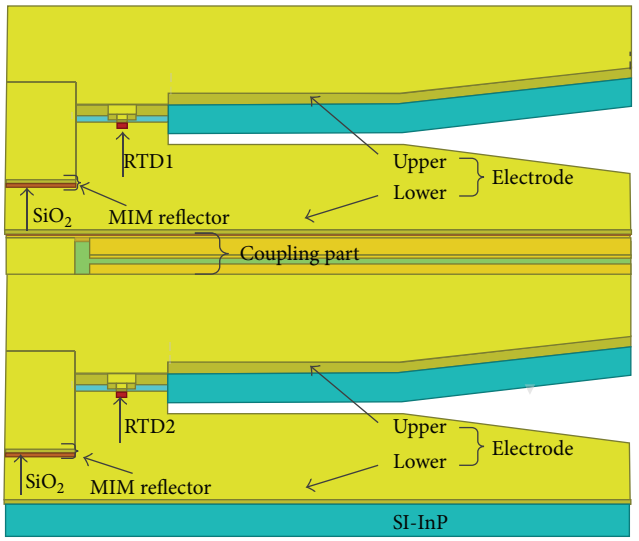

Figure 8: Schematic structure of the proposed TSA array integrated with RTDs.

The slot width $w3$ is 10 μm in the lower electrode, which is used for bias separation.

The oscillation modes of the two-element RTD oscillators array can be divided into the even mode and the odd mode when RTD_1 and RTD_2 are operated simultaneously. Two RTDs are assumed to be the same. The oscillation frequency of the even mode $\omega^{(e)}$ and the odd mode $\omega^{(o)}$ can be obtained as [28]

$$\omega = \omega^{(e)} \text{ and } \omega^{(o)} = \omega_1 \left[\sqrt{1 + \left(\frac{\omega_1 L}{2} \operatorname{Im}(Y_{12}) \right)^2} \mp \frac{\omega_1 L}{2} \operatorname{Im}(Y_{12}) \right], \quad (7)$$

where ω_1 is the angular frequency when RTD_1 is operated solely. L is the inductance mainly determined by the antenna

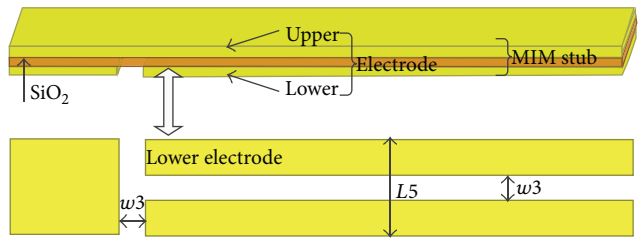

Figure 9: Schematic structure of the coupling part.

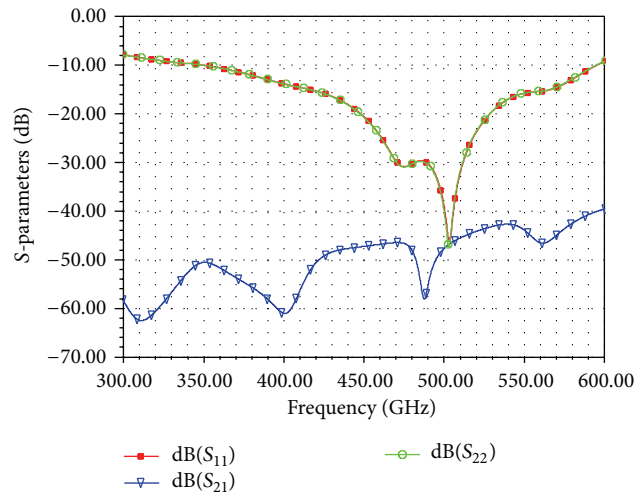

Figure 10: S-Parameters versus frequency of the proposed TSA array.

and the coupling part, and Y_{12} represents the coupling characteristic. If $\operatorname{Im}(Y_{12}) > 0$, the frequency of the even mode is lower than the other, and only this mode is stable.

The combined output power of the two-element RTD oscillators array in the even mode and odd mode is proportional to

$$|X_1 + X_2|^2 = \begin{cases} 4(1 + \operatorname{Re}(\kappa)), & \text{even mode,} \\ 0, & \text{odd mode,} \end{cases} \quad (8)$$

where X_n is the normalized complex amplitudes, which satisfies $|X_n|^2 = 1$, and κ is the coupling parameter given as

$$\kappa = -\frac{Y_{12}}{(a - G_L)}, \qquad a = \left(\frac{3}{2}\right)\left(\frac{\Delta I}{\Delta V}\right), \quad (9)$$

where G_L is the conductance determined by the antenna and coupling part. It can be seen from (8) that the combined output power of the two-element RTD oscillators array is about four times of a single oscillator in the even mode, while zero in the odd mode.

The S-parameters versus frequency of the proposed array is shown in Figure 10. We can observe that S_{11} and S_{22} are nearly coincident; besides, the S_{21} is below −40 dB, which

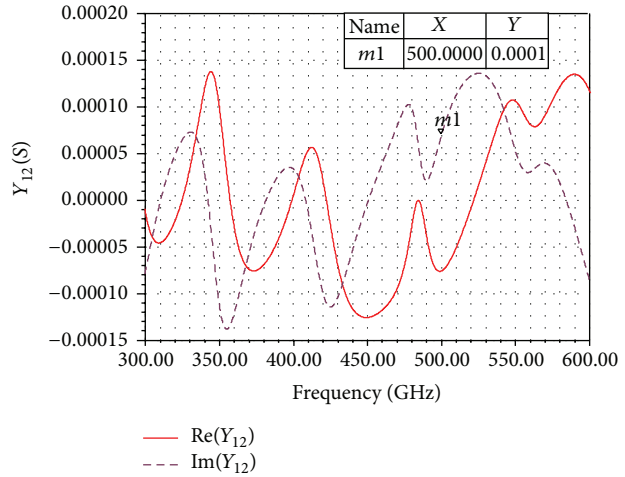

Figure 11: Admittance Y_{12} versus frequency of the proposed TSA array.

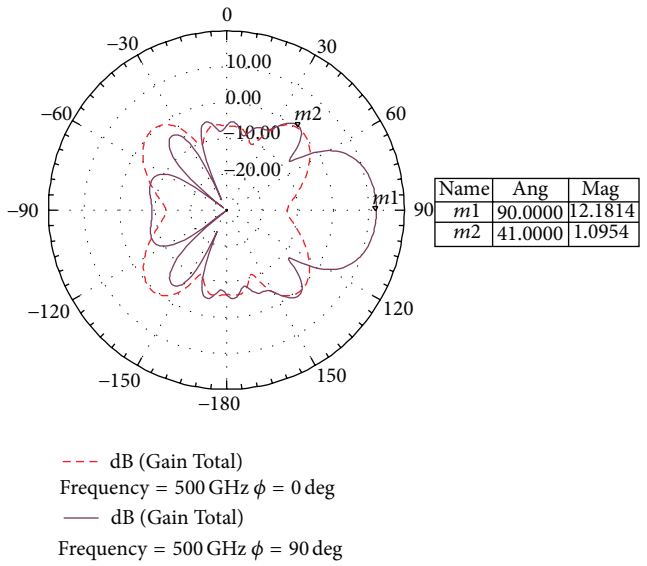

Figure 12: Radiation pattern of the proposed TSA array at 500 GHz.

means that the MIM stub works very well in reducing the mutual coupling between the TSA elements.

The admittance Y_{12} versus frequency of the proposed TSA array is shown in Figure 11. We can observe that the imaginary part of Y_{12} is positive; thus, the two-element RTD oscillators can work in the even mode and achieve the output power combination.

The radiation pattern of the proposed TSA array is shown in Figure 12. We can observe that the gain of the proposed TSA array is 12.18 dB at the horizontal direction, which is 2.6 dB larger than the gain of the TSA element. Furthermore, the first side lobe's gain is 1.1 dB at $\theta = 41^\circ$, and the front back to ratio is 21.3 dB. From the analysis of the radiation pattern of the TSA array, we can obtain that the TSA array enjoys a high gain at the horizontal direction, and the side lobes have been greatly suppressed.

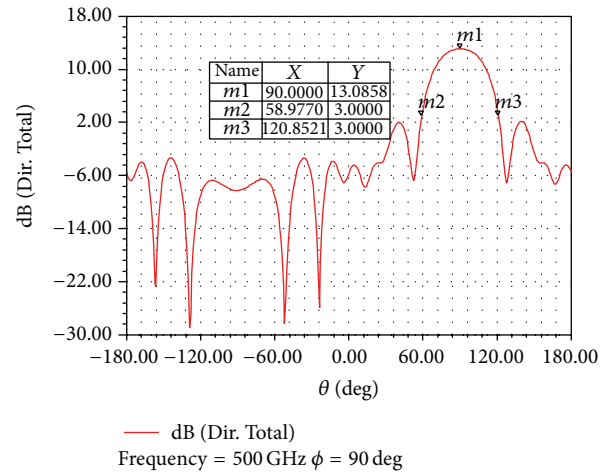

Figure 13: Directivity of the proposed TSA array at the E-plane at 500 GHz.

The directivity of the proposed TSA array at the E-plane at 500 GHz is shown in Figure 13. We can see that the maximum horizontal directivity is 13.09 dB, which is 2.71 dB larger than the directivity of the TSA element. Furthermore, the HPBW at the E-plane is 61°, which changes little compared with the HPBW of the TSA element. However, the beam width of the TSA array becomes narrower at the H-plane. Finally, the radiation efficiency of the TSA array is 81.2%, which means that the decrease of the radiation efficiency is quite little compared with the single TSA element. From the analysis of the directivity of the TSA array, we can conclude that the proposed TSA array has a very good directivity at the horizontal direction and hence can achieve the horizontal communication between the RTD oscillators and other integrated circuit chips.

5. Conclusion

The detailed modeling approaches and theoretical analysis of high directivity and high gain TSA array for THz RTD oscillators are presented in this paper. The MIM stub with a T-shaped slot is used to reduce the mutual coupling between the TSA elements. The simulation results show that the presented TSA element enjoys high directivity and high gain of 10.38 dB and 9.58 dB at the horizontal direction, respectively. When the two TSA elements formed to a linear array, the directivity and gain of the presented TSA array are 13.09 dB and 12.18 dB, which are 2.71 dB and 2.6 dB larger than that of the single TSA element, respectively. The S_{21} of the TSA array is below −40 dB, which means that the mutual coupling between the TSA elements has been greatly reduced. The first side lobe's gain is 1.1 dB; thus, the side lobes of the TSA array have been greatly suppressed. Finally, the radiation efficiency of the TSA array is 81.2%, which means that the decrease of the radiation efficiency is quite little compared with the TSA element. Therefore, the presented TSA array has the advantages of both the high directivity and high gain at the horizontal direction and hence can achieve

the horizontal communication between the RTD oscillators and other integrated circuit chips. The presented two-element TSA array can be extended to a multielement array. The presented analytical method and achieved performance are very promising for the antenna array integrated with the RTD oscillators at the THz frequency and could pave the way to the design of the THz antenna array for the RTD oscillators.

Conflict of Interests

The authors declare that there is no conflict of interests regarding the publication of this paper.

Acknowledgments

The authors wish to thank Professor W. L. Guo, School of Electronic Information Engineering, TianJin University, for his continuous encouragement and fruitful discussions. This work was supported by the National Natural Science Foundation of China (Grants nos. 61372011 and No. 61331003).

References

[1] M. Tonouchi, "Cutting-edge terahertz technology," *Nature Photonics*, vol. 1, no. 2, pp. 97–105, 2007.

[2] P. H. Siegel, "Terahertz technology," *IEEE Transactions on Microwave Theory and Techniques*, vol. 50, no. 3, pp. 910–928, 2002.

[3] T. Kleine-Ostmann and T. Nagatsuma, "A review on terahertz communications research," *Journal of Infrared, Millimeter, and Terahertz Waves*, vol. 32, no. 2, pp. 143–171, 2011.

[4] H.-J. Song and T. Nagatsuma, "Present and future of terahertz communications," *IEEE Transactions on Terahertz Science and Technology*, vol. 1, no. 1, pp. 256–263, 2011.

[5] E. R. Brown, J. R. Söderström, C. D. Parker, L. J. Mahoney, K. M. Molvar, and T. C. McGill, "Oscillations up to 712 GHz in InAs/AlSb resonant-tunneling diodes," *Applied Physics Letters*, vol. 58, no. 20, pp. 2291–2293, 1991.

[6] M. Reddy, S. C. Martin, A. C. Molnar et al., "Monolithic Schottky-collector resonant tunnel diode oscillator arrays to 650 GHz," *IEEE Electron Device Letters*, vol. 18, no. 5, pp. 218–221, 1997.

[7] M. Feiginov, C. Sydlo, O. Cojocari, and P. Meissner, "Resonant-tunnelling-diode oscillators operating at frequencies above 1.1 THz," *Applied Physics Letters*, vol. 99, no. 23, Article ID 233506, 2011.

[8] R. Sekiguchi, Y. Koyama, and T. Ouchi, "Subterahertz oscillations from triple-barrier resonant tunneling diodes with integrated patch antennas," *Applied Physics Letters*, vol. 96, no. 6, Article ID 0621153, pp. 1–3, 2010.

[9] N. Sashinaka, Y. Oguma, and M. Asada, "Observation of terahertz photon-assisted tunneling in triple-barrier resonant tunneling diodes integrated with patch antenna," *Applied Physics Letters*, vol. 39, no. 8, pp. 4899–4903, 2000.

[10] K. Hinata, M. Shiraishi, and S. Suzuki, "Sub-terahertz resonant tunneling diode oscillators with high output power (~200 μW) using offset-fed slot antenna and high current density," *Applied Physics Express*, vol. 3, no. 1, Article ID 014001, pp. 1–3, 2010.

[11] R. Janaswamy and D. H. Schaubert, "Analysis of the tapered slot antenna," *IEEE Transactions on Antennas and Propagation*, vol. 35, no. 9, pp. 1058–1065, 1987.

[12] I. K. Kim, N. Kidera, S. Pinel et al., "Linear tapered cavity-backed slot antenna for millimeter-wave LTCC modules," *IEEE Antennas and Wireless Propagation Letters*, vol. 5, no. 1, pp. 175–178, 2006.

[13] D. S. Woo, Y. G. Kim, and K. W. Kim, "Ultra-wideband millimeter-wave tapered slot antennas," in *Proceedings of the Antennas and Propagation Society International Symposium*, pp. 1969–1972, IEEE, Honolulu, Hawaii, USA, June 2007.

[14] I. Wood, D. Dousset, J. Bornemann, and S. Claude, "Linear tapered slot antenna with substrate integrated waveguide feed," in *Proceedings of the IEEE Antennas and Propagation Society International Symposium*, pp. 4761–4764, Honolulu, Hawaii, USA, June 2007.

[15] K. Urayama, S. Aoki, S. Suzuki, M. Asada, H. Sugiyama, and H. Yokoyama, "Sub-terahertz resonant tunneling diode oscillators integrated with tapered slot antennas for horizontal radiation," *Applied Physics Express*, vol. 2, no. 4, Article ID 044501, pp. 1–3, 2009.

[16] M. Asada, N. Orihashi, and S. Suzuki, "Voltage-controlled harmonic oscillation at about 1 THz in resonant tunneling diodes integrated with slot antennas," *Japanese Journal of Applied Physics*, vol. 46, no. 5A, pp. 321–324, 2007.

[17] S. Suzuki, A. Teranishi, K. Hinata, M. Asada, H. Sugiyama, and H. Yokoyama, "Fundamental oscillation of up to 831 GHz in GaInAs/AlAs resonant tunneling diode," *Applied Physics Express*, vol. 2, no. 5, Article ID 054501, pp. 1–3, 2009.

[18] M. Shiraishi, S. Suzuki, A. Teranishi, M. Asada, H. Sugiyama, and H. Yokoyama, "Fundamental oscillation up to 915GHz in InGaAs/AlAs resonant tunneling diodes integrated with slot antennas," in *Proceedings of the 34th International Conference on Infrared, Millimeter, and Terahertz Waves (IRMMW-THz '09)*, pp. 1–2, Busan, Republic of Korea, September 2009.

[19] S. Suzuki, M. Asada, A. Teranishi, H. Sugiyama, and H. Yokoyama, "Fundamental oscillation of resonant tunneling diodes above 1 THz at room temperature," *Applied Physics Letters*, vol. 97, no. 24, Article ID 242102, pp. 1–3, 2010.

[20] S. Suzuki and M. Asada, "Coherent power combination in highly integrated resonant tunneling diode oscillators with slot antennas," *Japanese Journal of Applied Physics, Part 2: Letters*, vol. 46, no. 45–49, pp. L1108–L1110, 2007.

[21] K. S. Yngvesson, T. L. Korzeniowski, Y.-S. Kim, E. L. Kollberg, and J. F. Johansson, "Tapered slot antenna-new integrated element for millimeter-wave applications," *IEEE Transactions on Microwave Theory and Techniques*, vol. 37, no. 2, pp. 365–374, 1989.

[22] K. S. Yngvesson, D. H. Schaubert, T. L. Korzeniowski, E. L. Kollberg, T. Thungren, and J. F. Johansson, "Endfire tapered slot antennas on dielectric substrates," *IEEE Transactions on Antennas and Propagation*, vol. 33, no. 12, pp. 1392–1400, 1985.

[23] S. Suzuki and M. Asada, "Proposal of resonant tunneling diode oscillators with offset-fed slot antennas in terahertz and sub-terahertz range," *Japanese Journal of Applied Physics, Part 1*, vol. 46, no. 1, pp. 119–121, 2007.

[24] N. Orihashi, S. Hattori, S. Suzuki, and M. Asada, "Experimental and theoretical characteristics of sub-terahertz and terahertz oscillations of resonant tunneling diodes integrated with slot antennas," *Japanese Journal of Applied Physics, Part 1*, vol. 44, no. 11, pp. 7809–7815, 2005.

[25] C. S. Kim and A. Brandli, "High-frequency high-power operation of tunnel diodes," *IRE Transactions on Circuit Theory*, vol. 8, no. 4, pp. 416–425, 1961.

[26] S. Suzuki, M. Shiraishi, H. Shibayama, and M. Asada, "High-power operation of terahertz oscillators with resonant tunneling diodes using impedance-matched antennas and array configuration," *IEEE Journal on Selected Topics in Quantum Electronics*, vol. 19, no. 1, Article ID 8500108, 2013.

[27] M. Asada, S. Suzuki, and N. Kishimoto, "Resonant tunneling diodes for sub-terahertz and terahertz oscillators," *Japanese Journal of Applied Physics*, vol. 47, no. 6, pp. 4375–4384, 2008.

[28] M. Asada and S. Suzuki, "Theoretical analysis of coupled oscillator array using resonant tunneling diodes in subterahertz and terahertz range," *Journal of Applied Physics*, vol. 103, no. 12, Article ID 124514, 2008.